The Large, Oxygen-Rich Halos of Star-Forming Galaxies Are A Major Reservoir of Galactic Metals

J. Tumlinson,[1][*] C. Thom,[1] J. K. Werk,[2] J. X. Prochaska,[2] T. M. Tripp,[3]
D. H. Weinberg,[4] M. S. Peeples,[5] J. M. O'Meara,[6] B. D. Oppenheimer,[7]
J. D. Meiring,[3] N. S. Katz,[3] R. Davé,[8] A. B. Ford,[8] K. R. Sembach[1]

[1]Space Telescope Science Institute, Baltimore, MD

[2]University of California Observatories-Lick Observatory, Santa Cruz, CA

[3]Department of Astronomy, University of Massachusetts, Amherst, MA

[4]Department of Astronomy, The Ohio State University, Columbus, OH

[5]Department of Physics and Astronomy, University of California, Los Angeles, CA

[6]Department of Chemistry and Physics, Saint Michael's College, Colchester, VT

[7]Leiden Observatory, Leiden University, the Netherlands

[8]Steward Observatory, University of Arizona, Tucson, AZ

[*]To whom correspondence should be addressed; E-mail: tumlinson@stsci.edu.

The circumgalactic medium (CGM) is fed by galaxy outflows and accretion of intergalactic gas, but its mass, heavy element enrichment, and relation to galaxy properties are poorly constrained by observations. In a survey of the outskirts of 42 galaxies with the Cosmic Origins Spectrograph onboard the Hubble Space Telescope, we detected ubiquitous, large (150 kiloparsec) halos of ionized oxygen surrounding star-forming galaxies, but we find much less ionized oxygen around galaxies with little or no star formation. This ionized CGM contains a substantial mass of heavy elements and gas, perhaps far exceeding the reservoirs of gas in the galaxies themselves. It is a basic component of nearly all star-forming galaxies that is removed or transformed during the quenching of star formation and the transition to passive evolution.

Galaxies grow by accreting gas from the intergalactic medium (IGM) and converting it to stars. Stellar winds and explosions release gas enriched with heavy elements (or metals, *1*), some of which is ejected in galactic-scale outflows (*2*). The circumgalactic medium (CGM),

loosely defined as gas surrounding galaxies within their own halos of dark matter (out to 100-300 kiloparsec), lies at the nexus of accretion and outflows, but the structure of the CGM and its relation to galaxy properties are still uncertain. Galactic outflows are observed at both low (*2-4*) and high (*5-7*) redshift, but it is unclear how far they propagate, what level of heavy-element enrichment they possess, and whether the gas escapes the halo or eventually returns to fuel later star formation. Models of galaxy evolution require significant outflows to explain observed galaxy masses and chemical abundances and to account for metals observed in the more diffuse IGM (*9,10*). The CGM may also reflect the theoretically-predicted transition from filamentary streams of cold gas that feed low mass galaxies to hot, quasi-static envelopes that surround high mass galaxies (*11, 12*). Both outflow and accretion through the CGM may be intimately connected to the observed dichotomy between blue, star-forming, disk-dominated galaxies and red, passively evolving, elliptical galaxies with little or no star formation (*13*). However, the low density of the CGM makes it extremely difficult to probe directly, thus models of its structure and influences are typically constrained indirectly by its effects on the visible portions of galaxies, not usually by observations of the gas itself.

We have undertaken a large program with the new Cosmic Origins Spectrograph (COS) aboard the Hubble Space Telescope to directly map the CGM using the technique of absorption-line spectroscopy, in which a diffuse gas is detected by its absorption of light from a background source. Our background sources are UV-bright quasi-stellar objects (QSOs), which are the luminous active nuclei of galaxies lying far behind the galaxies of interest. We focus on the ultraviolet 1032,1038 Å doublet of O VI (O^{+5}), the most accessible tracer of hot and/or highly ionized gas at redshift $z < 0.5$. O VI has been used to trace missing baryons in the IGM (*14-17*), the association of metals with galaxies (*18-20*), and coronal gas in the Milky Way halo (*21*).

The high sensitivity of COS enables a QSO absorption-line survey of halos around galaxies with a predetermined set of properties. We have selected 42 sample galaxies (Tables S1 and S2) that span redshifts $z_{\mathrm{gal}} = 0.10 - 0.36$, stellar masses $\log(M_*/M_\odot) = 9.5 - 11.5$. The QSO sightlines probe projected radial distances (i.e. impact parameters) to the galaxies of $R = 14 - 155$ kpc. We used the COS data to measure the O VI column densities (N_{OVI} in cm^{-2}), line profiles, and velocities with respect to the target galaxies (Fig. 1, SOM text S3-4). We measured precise redshifts, star formation rates (SFR in $M_\odot$ yr^{-1}), and metallicities for our sample galaxies using low-resolution spectroscopy from the Keck Observatory Low-Resolution Imaging Spectrograph (LRIS) and the Las Campanas Observatory Magellan Echellette (MagE) spectrograph (*22*, SOM text S2).

Our systematic sampling of galaxy properties allows us to investigate the connection between galaxies themselves and the CGM. The O VI detections extend to $R = 150$ kpc away from the targeted galaxies, but the whole sample shows no obvious trend with radius R (Fig. 2). The strong clustering of detections within $\pm$ 200 km s^{-1} of the galaxy systemic velocities indicates a close physical and/or gravitational association.

Circumgalactic medium gas as traced by O VI reflects the underlying bimodality of the general galaxy population (*13, 25*). We find a correlation of N_{OVI} with specific star formation rate sSFR ($\equiv$ SFR/M_*; Fig 3). For the 30 galaxies with sSFR $\geq 10^{-11}$ yr^{-1}, there are 27

detections with a typical column density $\log N_{\mathrm{OVI}} = 14.5$ (*23*) and a high covering fraction $f_{\mathrm{hit}} \approx 0.8 - 1$ maintained all the way to $R = 150\,\mathrm{kpc}$ (Fig. 2). For the 12 galaxies in the passive subsample ($\mathrm{sSFR} \leq 10^{-11}\,\mathrm{yr}^{-1}$) there are only 4 detections with lower typical N_{OVI} than the star-forming subsample (*26*). Accounting for the upper limits in N_{OVI} and sSFR, we can reject the null hypothesis that there is no correlation between N_{OVI} and sSFR at $> 99.9\%$ confidence for the whole sample and $> 98\%$ for each of the 50 kpc annuli shown in Figure 1 (SOM text S5). This effect remains even when we control for stellar mass: a Kolmogorov-Smirnov test over $\log M_* > 10.5$, where the star-forming and passive subsamples overlap, rejects at $> 99\%$ confidence the null hypothesis that they draw from the same parent distribution of N_{OVI} (Fig. S2). We therefore conclude that the basic dichotomy between star-forming ("blue-cloud") and passive ("red-sequence") galaxies is strongly reflected in their gaseous halos, and that the CGM out to at least 150 kpc either directly influences or is directly affected by star formation.

O VI is a fragile ionization state, which never exceeds a fraction $f_{\mathrm{OVI}} = 0.2$ of the total oxygen for the physical conditions of halo gas and is frequently much less abundant (Fig. 4). Our observations imply a typical CGM oxygen mass for star-forming galaxies of

$$M_{\mathrm{O}} = 5\pi R^2 \langle N_{\mathrm{OVI}} \rangle m_{\mathrm{O}} f_{\mathrm{hit}} \left(\frac{0.2}{f_{\mathrm{OVI}}} \right) = 1.2 \times 10^7 \left(\frac{0.2}{f_{\mathrm{OVI}}} \right) M_{\odot}\,, \tag{1}$$

where we have taken a typical $\langle N_{\mathrm{OVI}} \rangle = 10^{14.5}\,\mathrm{cm}^{-2}$ and $R = 150\,\mathrm{kpc}$, and the hit rate correction f_{hit} computed separately in three 50 kpc annuli (Figs. 1 and 2). This mass of oxygen is strictly a lower limit because we have scaled to the maximum $f_{\mathrm{OVI}} = 0.2$ (Fig. 4). The corresponding total mass of circumgalactic gas is

$$M_{\mathrm{gas}} = 177 \left(\frac{Z_{\odot}}{Z} \right) M_{\mathrm{O}} = 2 \times 10^9 \left(\frac{Z_{\odot}}{Z} \right) \left(\frac{0.2}{f_{\mathrm{OVI}}} \right) M_{\odot}\,, \tag{2}$$

where Z is the gas metallicity, and the solar oxygen abundance is $n_{\mathrm{O}}/n_{\mathrm{H}} = 5 \times 10^{-4}$ (*28*).

Even for the most conservative ionization correction ($f_{\mathrm{OVI}} = 0.2$), the OVI-traced CGM contains a mass of metals and gas that is substantial by comparison with other reservoirs of interstellar and circumgalactic gas. If our sample galaxies lie on the mean trend of gas fraction for low-z galaxies (*29*), they have interstellar medium (ISM) gas masses of $M_{\mathrm{ISM}} = (5 - 10) \times 10^9 M_{\odot}$ and contain $M_{\mathrm{ISM}}^{\mathrm{O}} = (2 - 10) \times 10^7 M_{\odot}$ of oxygen, taking into account the observed correlation between galaxy stellar mass and ISM metallicity (Fig. 4, SOM text S5). The minimum CGM oxygen mass is thus 10-70% of the ISM oxygen (Figs. 4 and S4). The covering fractions and column densities we find for star-forming galaxies are insensitive to M_*, while the ISM metal masses decline steeply with M_* according to the mass-metallicity relation. Thus the ratio of CGM metals to ISM metals appears to increase for lower mass galaxies (assuming constant f_{OVI}), perhaps indicating that metals more easily escape from their shallower gravitational potentials. The implied total mass of circumgalactic gas M_{gas} is more uncertain because it can strictly take on any metallicity; for a fiducial solar metallicity, Equation (2) implies a total CGM mass comparable to M_{ISM}, and several times the total mass inferred

3

for Milky Way "high velocity clouds" (HVCs) (*30, 31*) or for low-ionization (Mg II) gas filling halos to $R = 100$ kpc (*32*).

For the densities typically expected at radii $R \sim 100$ kpc, f_{OVI} exceeds 0.1 only over a narrow temperature range $10^{5.4-5.6}$ K, and it only exceeds 0.02 over $10^{5.2-5.7}$ K (Fig. 4). Either a large fraction of CGM gas lies in this finely tuned temperature range — a condition that is difficult to maintain because gas cooling rates peak at $T \approx 10^{5.5}$ K — or the CGM oxygen and gas masses are much larger than the minimum values we have quoted above. Lower density, photoionized gas can achieve high $f_{\mathrm{OVI}} \sim 0.1$ over a wider temperature range, but at these low densities it is hard to produce a $10^{14.5}\,\mathrm{cm}^{-2}$ column density within the confines of a galactic halo, especially if the metallicity is low (Fig. S5). Thus $f_{\mathrm{OVI}} = 0.02$ and $Z = 0.1 Z_\odot$ are plausible conditions for the O VI-traced gas, but it is unlikely that both conditions hold simultaneously. However, if either one holds the CGM detected here could represent an important contribution to the cosmic budgets of metals and baryons. In either case M_{gas} is comparable to the total $\sim 3 \times 10^{10} M_\odot$ inside $R = 300$ kpc inferred from H I measurements at low redshift (*20*), and the $\sim 4 \times 10^{10} M_\odot$ inferred for the CGM surrounding rapidly star-forming galaxies at $z \approx 2 - 3$ (*8*). By generalizing our typical M_{O} to all star-forming galaxies with $M_* > 10^{9.5} M_\odot$, we estimate that the halos of such galaxies contain $15\% \times (0.02/f_{\mathrm{OVI}})$ of the oxygen in the universe and $2\% \times (0.02/f_{\mathrm{OVI}}) \times (Z_\odot/Z)$ of the baryons in the universe.

The metals detected out to $R \sim 150$ kpc must have been produced in galaxies, after which they were likely transported into the CGM in some form of outflow. However, these outflows need not be active at the time of observation; indeed the large masses imply long timescales. Because 1 $M_\odot$ of star formation eventually returns 0.014 $M_\odot$ of oxygen to the ISM (*33*), at least $8.6 \times 10^8 M_\odot$ of star formation is required to yield the detected oxygen mass. This is equivalent to $\sim 3 \times 10^8$ yr of star formation at the median SFR $= 3\,M_\odot\,\mathrm{yr}^{-1}$ of our star-forming sample, in the unlikely event that all oxygen produced is expelled to the CGM, and longer in inverse proportion to the fraction of metals retained in the ISM. Thus the detected oxygen could be the cumulative effect of steady enrichment over the preceding several Gyr, the product of sporadic flows driven by rapid starbursts and an active nucleus (*34*), or the fossil remains of outflows from as early as $z \sim 1.5 - 3$ (*7, 8*). While the exact origin of the mass-metallicity relation of galaxies is not yet known, models that explain it in terms of preferential loss of metals imply that a substantial fraction of the metals produced by star formation must be ejected from the galaxy rather than retained in the ISM (*29*). The CGM detected here could be a major reservoir of this ejected material, with important consequences for models of galactic chemical evolution.

The O VI we observe arises in bulk flows of gas over $100 - 400$ km s^{-1}, but the relative velocities are usually below halo escape speeds (Fig. 2), even when we take projection effects into account (Fig. S1). Thus much of the material driven into the halo by star formation could eventually be reacquired by the galaxy in "recycled winds," which may be an important source of fuel for ongoing star formation (*35*). It is unlikely that the detected gas is predominantly fresh material accreting from the IGM because models of "cold mode" accretion predict very low metallicity and low covering fractions $f_{\mathrm{hit}} \sim 10 - 20\%$ (*36, 37*), and "hot mode" accretion typically involves gas at temperatures $T > 10^6$ K with undetectably low f_{OVI}.

The passive galaxies in our sample once formed stars, thus it follows that they would once have possessed halos of ionized, metal-enriched gas visible in O VI. The relative paucity of O VI around these galaxies implies that this material was transformed by processes that plausibly accompany the quenching of star formation (*38*), such as tidal stripping in group environments, re-accretion onto the galaxy in ionized form, or heating or cooling to a temperature at which O VI is too rare to detect. Our findings present a quantitative challenge for theoretical models of galaxy growth and feedback, which must explain both the ubiquitous presence of massive, metal-enriched ionized halos around star-forming galaxies and the fate of these metals after star formation ends.

References and Notes

1. In astronomical usage, metals are those elements heavier than hydrogen and helium that are formed only by stellar nucleosynthesis.

2. S. Veilleux, G. Cecil, G., & J. Bland-Hawthorn, *Ann. Rev. Astron. & Astrophys.*, **43**, 769 (2005).

3. M. D. Lehnert, & T. M. Heckman, *Astrophys. J.*, **462**, 651 (1996).

4. C. L. Martin, *Astrophys. J.* **621**, 227 (2005).

5. D. S. Rupke, S. Veilleux, & D. B. Sanders, *Astrophys. J. Suppl. Ser.*, **160**, 115 (2005).

6. A. E. Shapley, C. C. Steidel, M. Pettini, & K. L. Adelberger, *Astrophys. J.*, **588**, 65 (2003).

7. B. J. Weiner, et al., *Astrophys. J.*, **692**, 187 (2009).

8. C. C. Steidel, et al., *Astrophys. J.* **717**, 289 (2010).

9. V. Springel, & L. Hernquist, *Mon. Not. R. Astron. Soc.*, **339**, 312 (2003).

10. B. D. Oppenheimer, & R. Davé, *Mon. Not. R. Astron. Soc.*, **373**, 1265 (2006).

11. D. Kereš, N. Katz, D. H. Weinberg, & R. Davé, *Mon. Not. R. Astron. Soc.*, **363**, 2 (2005).

12. A. Dekel, & Y. Birnboim, *Mon. Not. R. Astron. Soc.*, **368**, 2 (2006).

13. G. Kauffmann, et al., *Mon. Not. R. Astron. Soc.*, **341**, 33 (2003).

14. T. M. Tripp, B. D. Savage, & E. B. Jenkins, *Astrophys. J. Lett.*, **534**, L1 (2000).

15. C. W. Danforth, & J. M. Shull, *Astrophys. J.* **679**, 194 (2008).

16. C. Thom, & H.-W. Chen, *Astrophys. J.* **683**, 22 (2008).

17. J. N. Bregman, *Ann. Rev. Astron. Astro.*, **45**, 221 (2007).

18. J. T. Stocke, et al., *Astrophys. J.* **641**, 217 (2006).

19. H.-W. Chen, & J. S. Mulchaey, *Astrophys. J.* **701**, 1219 (2009).

20. J. X. Prochaska, B. Weiner, H.-W. Chen, J. S. Mulchaey, & K. L. Cooksey, http://arxiv.org/abs/1103.1891 (2011).

21. K. R. Sembach, et al., *Astrophys. J. Suppl. Ser.* **146**, 165 (2003).

22. J. K. Werk, et al., http://arxiv.org/abs/1108.3852 (2011).

23. The typical $\log N_{\rm OVI} = 14.5 - 15.0$ for star-forming galaxies resembles the high end of the column-density distribution seen in blind surveys of intergalactic clouds (*15, 16, 24*) and is higher than the mean value (14.0) measured by the Far Ultraviolet Spectroscopic Explorer through the halo of the Milky Way (*21*), which would belong in our star-forming sample.

24. T. M. Tripp, et al., *Astrophys. J. Suppl. Ser.* **177**, 39 (2008).

25. D. Schiminovich, et al., *Astrophys. J. Suppl. Ser.* **173**, 315 (2007).

26. O VI *emission* is seen in elliptical galaxies (*27*), but this gas is most likely associated with the ISM and not the CGM.

27. J. N. Bregman, E. D. Miller, A. E. Athey, & J. A. Irwin, *Astrophys. J.*, **635**, 1031 (2005).

28. M. Asplund, N. Grevesse, A. J. Sauval, & P. Scott, *Ann. Rev. Astron. & Astrophys.*, **47**, 481 (2009).

29. M. S. Peeples, & F. Shankar, http://arxiv.org/abs/1007.3743 (2010).

30. M. E. Putman, *Astrophys. J.*, **645**, 1164 (2006).

31. N. Lehner, & J. C. Howk, Science Express, science.1209069, (2011).

32. H.-W. Chen, et al., *Astrophys. J.*, **714**, 1521 (2010).

33. D. Thomas, L. Greggio, & R. Bender, *Mon. Not. R. Astron. Soc.*, **296**, 119 (1998).

34. Tripp, T. M., et al., *Science*, submitted (2011).

35. B. D. Oppenheimer, et al., *Mon. Not. R. Astron. Soc.*, **406**, 2325 (2010).

36. K. R. Stewart, et al., *Astrophys. J. Lett.*, **735**, L1 (2011).

37. M. Fumagalli, et al., http://arxiv.org/abs/1103.2130 (2011).

38. J. M. Gabor, R. Davé, K. Finlator, & B. D. Oppenheimer, *Mon. Not. R. Astron. Soc.*, **407**, 749 (2010).

39. D. P. Schneider, *et al.*, *Astron. J.* **134**, 102 (2007).

40. http://galex.stsci.edu/GR4/

41. S. Osterman, et al., *Astrophys & Space Sci.*, **157** (2011).

42. J. Tumlinson, et al., *Astrophys. J.*, **733**, 111 (2011).

43. J. D. Meiring, et al., *Astrophys. J.*, **732**, 35 (2011).

44. http://www.ucolick.org/∼xavier/LowRedux/index.html

45. http://web.mit.edu/jjb/www/MASE.html

46. M. R. Blanton, & S. Roweis, *Astron. J.*, **133**, 734 (2007).

47. E. F. Bell, D. H. McIntosh, N. S. Katz, & M. D. Weinberg, *Astrophys J. Supp. Ser.*, **149**, 289 (2003).

48. D. H. McIntosh, et al., *Mon. Not. R. Astron. Soc.*, **388**, 1537 (2008).

49. J. Dunkley, et al., *Astrophys. J. Supp. Ser.*, **180**, 306 (2009).

50. D. J. Schlegel, D. P. Finkbeiner, & M. Davis, *Astrophys. J.*, **500**, 525 (1998).

51. J. A. Cardelli, G. C. Clayton, & J. S. Mathis, *Astrophys. J.*, **345**, 245 (1989).

52. R. C. Kennicutt, Jr., *Astrophys. J.*, **498**, 541 (1998).

53. D. G. Hummer, & P. J. Storey, *Mon. Not. R. Astron. Soc.*, **224**, 801 (1987).

54. B. D. Savage, & K. R. Sembach, *Astrophys. J.*, **379**, 245 (1991) .

55. P. Ghavamian, et al., COS ISR 2009-01, STScI (2009).

56. T. Isobe, E. D. Feigelson, & P. I. Nelson, *Astrophys. J.*, **306**, 490 (1986).

57. B. P. Moster, et al., *Astrophys. J.*, **710**, 903 (2010).

58. H.-W. Chen, K. M. Lanzetta, & J. K. Webb, *Astrophys. J.*, **556**, 158 (2001).

59. G. J. Ferland, et al., *Pub. Astron. Soc. Pac.*, **110**, 761 (1998).

60. Haardt, F. & Madau, P., in "Clusters of galaxies and the high redshift universe observed in X-rays, Recent results of XMM-Newton and Chandra", XXXVIth Rencontres de Moriond, eds. D.M. Neumann & J.T.T. Van (2001).

61. M. Fukugita, C. J. Hogan, & P. J. E. Peebles, *Astrophys. J.*, **503**, 518 (1998).

Supporting Online Material:
SOM Text
Figs. S1 to S5
Tables S1 and S2
References (39-61)
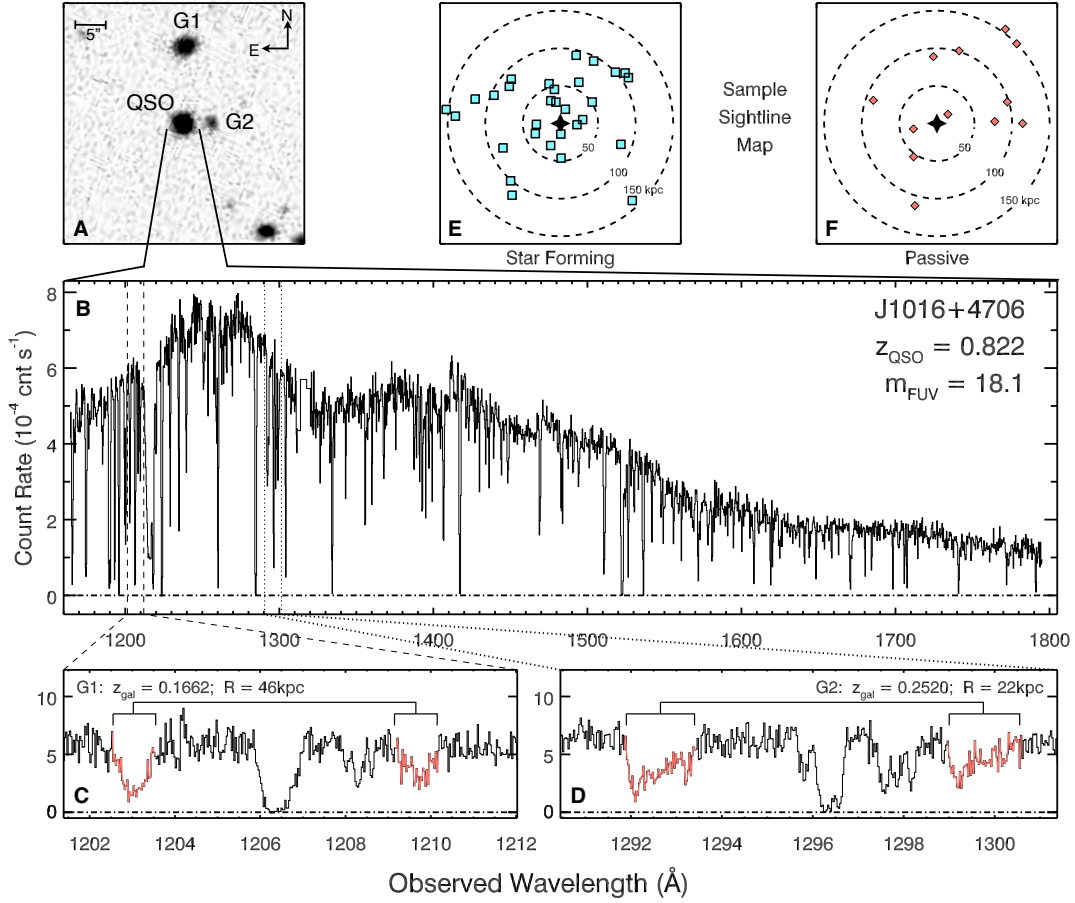
Figure 1: An illustration of our sampling technique and data. (**A**) An SDSS composite image of the field around the QSO J1016+4706 with two targeted galaxies, labeled G1 and G2, which are both in the star-forming subsample. (**B**) The complete COS count-rate spectrum (counts s^{-1}) versus observed wavelength. The panels below concentrate on the redshifted O VI 1032,1038 Å doublet for galaxies G1 (**C**) and G2 (**D**). The upper right panels illustrate the full sample by showing the locations of all sightlines in position angle and impact parameter R with respect to the targeted galaxies, for the star-forming (**E**) and passively evolving (**F**) subsamples. The circles mark $R = 50$, 100, and 150 kpc.
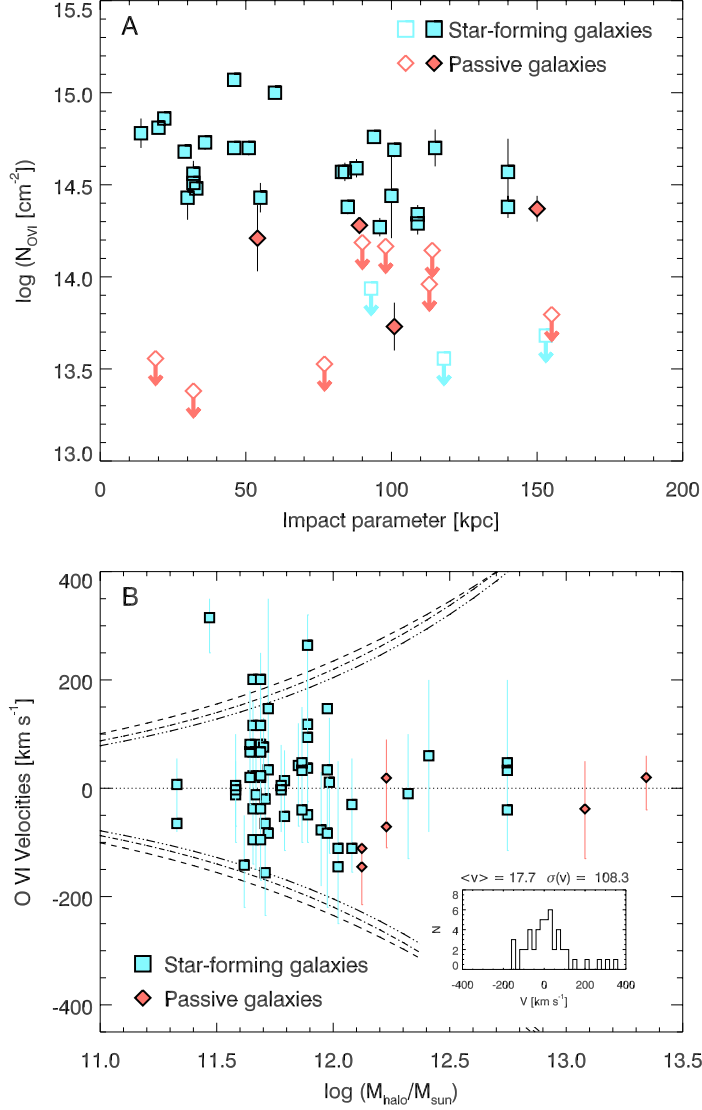
Figure 2: O VI association with galaxies. (**A**) O VI column density, N_{OVI} in cm^{-2}, vs. R in kiloparsec for the star-forming (blue) and passive (red) subsamples. Filled and open symbols mark O VI detections and 3σ upper limits, respectively. The detections in the star-forming galaxies maintain $\log N_{OVI} \sim 14.5$ to $R \sim 150$ kpc, the outer limit of our survey. (**B**) Component centroid velocities with respect to galaxy systemic redshift for O VI detections, versus inferred dark-matter halo mass. The range bars mark the full range of O VI absorption for each system. The inset shows a histogram of the component velocities. The dashed lines mark the mass-dependent escape velocity at $R = 50, 100,$ and 150 kpc from outside to inside.
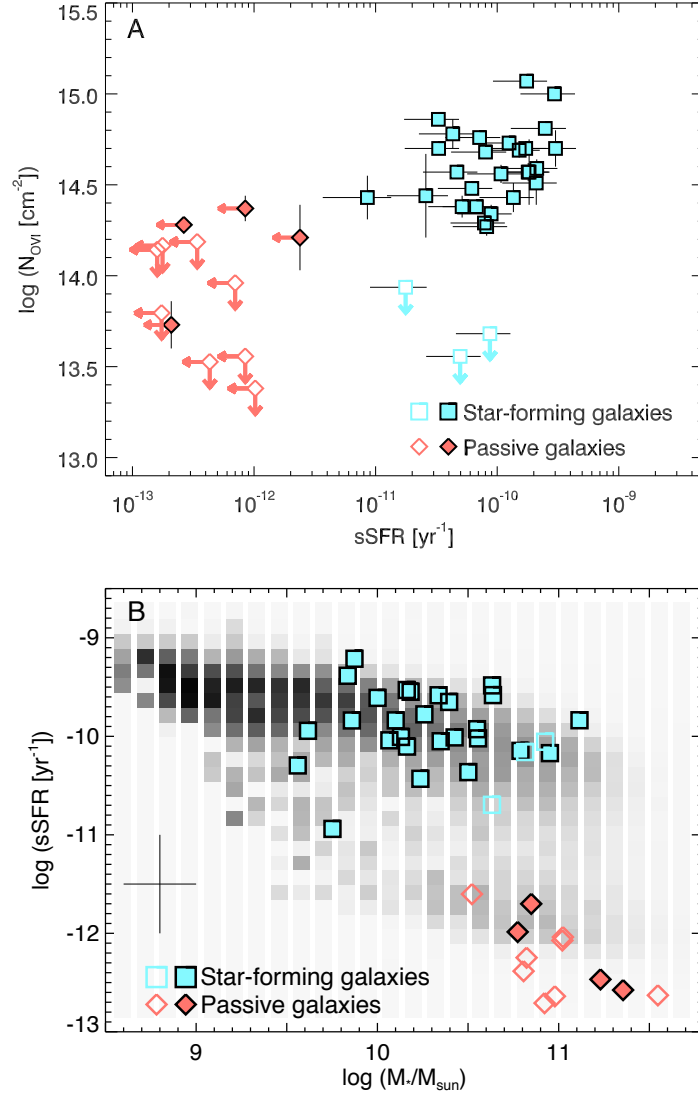
Figure 3: O VI correlation with galaxy properties. (**A**) O VI column density versus sSFR ($\equiv M_*/SFR$). Star-forming galaxies are divided from passively evolving galaxies by sSFR $\approx 10^{-11}$ yr^{-1}, our detection limit is sSFR $\sim 5 \times 10^{-12}$ yr^{-1}). (**B**) The galaxy color-magnitude diagram (sSFR versus M_*) for SDSS+GALEX galaxies from (*25*).
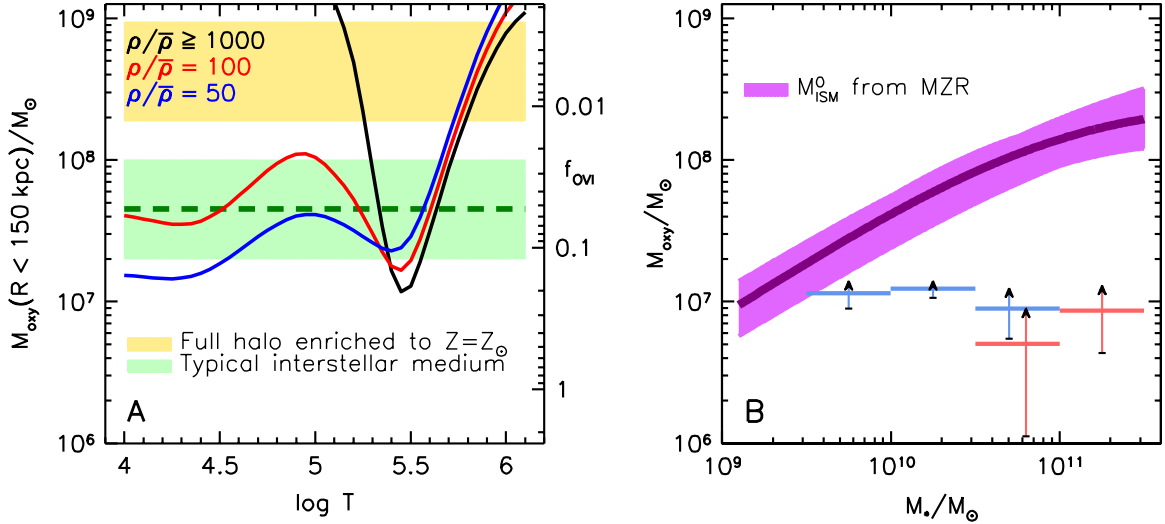
Figure 4: CGM oxygen masses compared to galactic reservoirs. (**A**) The curves and the axis labels at right show the fraction of gas-phase oxygen in the O VI ionization state f_{OVI} as a function of temperature, for three overdensities relative to the cosmic mean, $\rho/\bar{\rho}$. All $\rho/\bar{\rho} \geq 1000$ track the black curve on which collisional ionization dominates, while for lower values photoionization by the extragalactic background can increase f_{OVI} at low T. For gas that traces dark matter, $\rho/\bar{\rho} = 1000$ is typical at $R \approx 100$ kpc, while $\rho/\bar{\rho} = 50 - 100$ for the outskirts of the halo. The pale green band shows the expected oxygen mass of the galaxies' ISM if they lie on the standard relation between M_{ISM} and M_* and follow the mass-metallicity relation (MZR). The green dashed line shows the oxygen mass produced by $3 \times 10^9 M_\odot$ of star formation. The yellow band shows the expected oxygen mass for the extreme assumption that the typical host dark-matter halos ($2 \times 10^{11} - 10^{12} M_\odot$) have the universal baryon fraction and solar metallicity. (**B**) The CGM oxygen masses compared with the interstellar oxygen mass as a function of M_*. Points with range bars show the CGM oxygen mass M_O implied by Equation (1) for $f_{OVI} = 0.2$, calculated separately for star-forming (blue) and passive (red) galaxies according to the hit rates in four bins of stellar mass. The purple curves show the calculated M_{ISM}^O for typical star forming galaxies in the SDSS, accounting for the mean MZR in the central curve and its uncertainties in the shaded region. The data points increase their mass in inverse proportion to f_{OVI}.